

OPEN ACCESS

EDITED BY
Minhao Xie,
Naniing University of Finance as

Nanjing University of Finance and Economics, China

REVIEWED BY

Yuting Cui,

Affiliated Hospital of Nanjing University of Chinese Medicine, China Lining Wang,

China Academy of Chinese Medical Sciences, China

*CORRESPONDENCE
Zhihua Guo

☑ 004294@hnucm.edu.cn

RECEIVED 01 August 2025 ACCEPTED 06 October 2025 PUBLISHED 26 November 2025

CITATION

Shi M, Yuan H, Liu C, Wei J, Wang Z, Huang A, Zeng Q, Li Y and Guo Z (2025) Yixintai treats chronic heart failure in rats by regulating gut microbiota and bile acid. *Front. Microbiol.* 16:1672313. doi: 10.3389/fmicb.2025.1672313

COPYRIGHT

© 2025 Shi, Yuan, Liu, Wei, Wang, Huang, Zeng, Li and Guo. This is an open-access article distributed under the terms of the Creative Commons Attribution License (CC BY). The use, distribution or reproduction in other forums is permitted, provided the original author(s) and the copyright owner(s) are credited and that the original publication in this journal is cited, in accordance with accepted academic practice. No use, distribution or reproduction is permitted which does not comply with these terms.

Yixintai treats chronic heart failure in rats by regulating gut microbiota and bile acid

Min Shi^{1,2}, Hui Yuan³, Chengxin Liu⁴, Jiaming Wei^{1,2}, Ziyan Wang³, Aisi Huang¹, Qinghua Zeng¹, Ya Li⁵ and Zhihua Guo^{1,2,3}*

¹Hunan University of Chinese Medicine, Changsha, China, ²Provincial Key Laboratory of TCM Diagnostics, Hunan University of Chinese Medicine, Changsha, China, ³First Clinical College of Chinese Medicine, Hunan University of Chinese Medicine, Changsha, China, ⁴The Second Clinical College of Chinese Medicine, The Second Affiliated Hospital of Hunan University of Chinese Medicine, Changsha, China, ⁵School of Pharmacy, Hunan University of Chinese Medicine, Changsha, China

Introduction: Yixintai (YXT) medicine for chronic heart failure (CHF), has demonstrated safety and efficacy in the treatment of CHF. However, its precise mechanistic actions require further elucidation.

Methods: This study identified components in YXT using the UHPLC-QE-MS technique. A rat CHF model was created by ligating the left anterior descending coronary artery and an inflammatory injury model was induced in H9c2 cells using lipopolysaccharide (LPS) to evaluate the efficacy of YXT. After YXT treatment, changes in fecal gut microbiota and serum BAs profiles in rats were evaluated utilizing 16S rRNA sequencing and UHPLC-MS/MS techniques. Additionally, western blot (WB) and polymerase chain reaction (PCR) assays were conducted to assess the expression levels of TGR5 in both myocardial tissue and H9c2 cells. Cyclic adenosine monophosphate (cAMP), B-type natriuretic peptide (BNP), interleukin-1 beta (IL-1 β), interleukin-6 (IL-6), and tumor necrosis factoralpha (TNF- α) levels were also measured using enzyme-linked immunosorbent assay (ELISA).

Results: In total, 1049 components were identified in YXT. YXT treatment effectively attenuated the inflammatory reaction, reduced serum BNP levels, alleviated the pathological changes in the colon and myocardium, and improved cardiac function in CHF rats. YXT treatment significantly improved gut microbiota diversity in CHF rats, enhancing beneficial bacterial populations and serum bile acid levels, while reducing the abundance of detrimental bacteria. Furthermore, YXT treatment enhanced TGR5 expression in the myocardial tissue and H9c2 cells of CHF rats.

Discussion: These findings suggest that YXT exerts its therapeutic benefits by reshaping the gut microbiota, modulating bile acid metabolism, and activating TGR5.

KEYWORDS

chronic heart failure, Yixintai, gut microbiota, bile acid, TGR5

1 Introduction

Chronic heart failure (CHF) is a long-term condition that can stabilize, worsen, or lead to decompensation. As a severe outcome of various cardiovascular disorders, CHF manifests through dyspnea, fatigue, and fluid retention. The substantial disease burden of CHF, driven by its elevated rates of morbidity and mortality, underscores its global healthcare challenge (Baman and Ahmad, 2020). Afflicting more than 60 million individuals worldwide, heart failure (HF) represents a pervasive clinical entity that severely compromises daily functioning and wellbeing. Demographic aging and increasing chronic illnesses have contributed to escalating HF incidence (Savarese et al., 2023).

Heart failure poses a considerable risk to human health, often leading to poor prognoses and elevated mortality rates. Over 56 million people globally have HF, with a five-year survival rate below 50% post-diagnosis. As populations age and new treatments prolong life, HF cases are expected to increase by 46% by 2030, heavily straining healthcare systems. Despite a decline in overall HF mortality over the past decade, the fiveyear mortality rate is still a concerning 75% (Khan et al., 2024). While modern medicine has made notable strides in the prevention and management of CHF, prolonged use of pharmacological therapies can lead to various challenges, including adverse drug reactions and reduced quality of life. Furthermore, the lack of personalized treatment strategies and the relatively simplistic targeting of conventional therapies have emerged as notable limitations (Wohlfahrt et al., 2023; Bonfioli et al., 2025). Traditional Chinese Medicine (TCM)'s multi-target, multi-pathway approach has shown efficacy in improving symptomatic relief, functional capacity, and life quality in CHF (Wang et al., 2017). YXT, a traditional Chinese herbal formulation, has shown promising clinical efficacy in managing CHF, with its safety and therapeutic potential thoroughly validated through extensive research (Wang et al., 2024). YXT comprises herbal ingredients such as Astragalus membranaceus, Salvia miltiorrhiza, and Carthamus tinctorius, which are rich in bioactive compounds with therapeutic potential properties CHF. Genistein and formononetin are the primary effective components in YXT for treating HF. Research indicates that these compounds can markedly alleviate HF symptoms post-myocardial infarction and enhance cardiac function and ultrastructural integrity (Sangeethadevi et al., 2022; Wang M. N. et al., 2022; Wang X. et al., 2022).

The gut microbiota is integral to digestion and nutrient assimilation, providing essential energy to the host. Moreover, it functions as an endocrine organ, generating bioactive compounds and metabolites, including bile acid (BA), short-chain fatty acids

Abbreviations: BA, bile acid; BNP, B-type natriuretic peptide; BSH, bile salt hydrolase; CA, cholic acid; cAMP, cyclic adenosine monophosphate; CDCA, chenodeoxycholic acid; CHF, chronic heart failure; DCA, deoxycholic acid; EF, ejection fraction; ELISA, enzyme linked immunosorbent assay; FXR, farnesoid X receptor; HF, heart failure; HE, hematoxylin and eosin; IL-1β, interleukin-1 beta; IL-6, interleukin-6; LCA, lithocholic acid; LPS, lipopolysaccharide; PCR, polymerase chain reaction; PCoA, principal coordinates analysis; PXR, pregnane X receptor; SCFAs, short-chain fatty acids; SXR, steroid and xenobiotic receptor; TCM, traditional Chinese medicine; TGR5,Takeda G protein-coupled receptor 5; TMAO, trimethylamine N-oxide; TNF-α, tumor necrosis factor-alpha; UDCA, ursodeoxycholic acid; WB, western blot; YXT, YixinTai.

(SCFAs), and trimethylamine oxide (TMAO). These metabolites are crucial for metabolic processes and influence numerous physiological and pathological pathways (Tang et al., 2019; Yu et al., 2023). According to the 'gut hypothesis,' the gut microbiota is vital in managing CHF conditions (Nagatomo and Tang, 2015). In CHF, conditions such as ischemia, hypoxia, and edema can impair the intestinal lining, resulting in increased permeability and dysbiosis. This imbalance facilitates bacterial translocation, endotoxemia, and the cascade of pro-inflammatory mediators, which triggers systemic inflammation. Such inflammation adversely affects vascular endothelial function, impedes blood flow, disrupts nutrient supply, and contributes to multi-organ dysfunction, worsening CHF progression. Furthermore, the dynamic interplay between the host and gut microbiota is essential for BA metabolism and signaling, which are crucial for sustaining metabolic health (Nie et al., 2015; Chen et al., 2020). A recent study exploring the link between BA and cardiac function suggests that these compounds are significantly involved in CHF (Mayerhofer et al., 2017). Evidence has also shown that serum BA levels in CHF patients markedly differ from those in healthy individuals, suggesting that alterations in the gut microbiota-BA axis could play a role in the development of CHF (Winston and Theriot, 2020). BA regulate cardiovascular function by serving as signaling molecules, interacting with G protein-coupled receptors, including Takeda G protein-coupled receptor 5 (TGR5), and nuclear receptors such as the farnesoid X receptor (FXR) and pregnane X receptor/steroid and xenobiotic receptor (PXR/SXR) (Tang et al., 2019). Activation of cell surface receptor TGR5 by BA has been demonstrated to trigger protective responses in cardiac cells. In murine models, such effects enhance myocardial sensitivity to stimuli, boost contractility, and promote hemodynamic adaptation (Lugman et al., 2024).

To established a CHF model, rats underwent left anterior descending coronary artery ligation combined with a restricted diet. An inflammatory injury model was also induced in H9c2 cells using lipopolysaccharide (LPS). We investigated YXT's cardioprotective mechanisms, focusing on its effects on gut microbiota and related BA metabolites in CHF rats.

2 Materials and methods

2.1 Drug preparation and analysis

YixinTai (YXT) comprises eight TCM herbs, sourced from EFONG Pharmaceutical Ltd., in (Guangdong, China). The herbs included in this formulation are Huangqi (Astragalus membranaceus (Fisch.) Bunge, Cat. No. 1051693), Danshen (Salvia miltiorrhiza Bunge, Cat. No. 1080473), Honghua (Carthamus tinctorius L, Cat. No. 1081223), Renshen (Panax ginseng C. A. Mey, Cat. No. 1042233), Zexie (Alisma plantago-aquatica L, Cat. No. 1081173), Fuling (Poria cocos (Schw) Wol, Cat. No. 1071523), Zhuling (Polyporus umbellatus (Pers.) Fr, Cat. No. 1051953), and Tinglizi (Draba nemorosa L. (Cat. No. 1042123).

Sprague-Dawley (SD) rats (n = 10) were randomized into control or YXT-treated (5.6 g/kg/day) groups. After 10 days, blood was collected via abdominal aorta under pentobarbital anesthesia. Serum was isolated, heat-inactivated (56 °C, 30 min), and stored

at -80° C. YXT samples were homogenized in boiling water, vortexed, and centrifuged. Supernatant (300 μ L) was mixed with methanol:water (4:1, containing IS), vortexed, sonicated (ice-bath), then stored at -40° C (1 h). After centrifugation and filtration (0.22 μ m), QC aliquots were stored at -80° C. Samples were analyzed using UPLC (BEH C18 column; 0.1% formic acid mobile phase; 5 μ L injection) with gradient elution (85% \rightarrow 25% A in 11 min). MS (Q Exactive) operated in FullScan-ddMS2 mode (70,000/17,500 resolution; \pm 4.0/-3.6 kV spray voltage). Data were processed via XCMS (peak alignment, feature extraction) and annotated using MS/MS matching against a custom database.

2.2 Establishment and group treatment of a CHF rat model

Sixty SD rats were randomly allocated into two groups: the sham surgery group (n = 10) and the ligation group (n = 50). Anesthesia was induced with 2% sodium pentobarbital at a dose of 0.28 mL per 100 g body weight (Merck KGaA, Cat. No. P3761) to facilitate left anterior descending coronary artery ligation (Samsamshariat et al., 2005). The Sham group underwent the same surgical procedure without ligation. Postsurgery electrocardiograms confirmed successful ligation with elevated ST-T segments in the thoracic lead. Rats with successful ligation were placed on dietary restriction to establish the CHF model. After 4 weeks, cardiac ultrasound measurements revealed a left ventricular ejection fraction (EF) of 50%, confirming the successful induction of the CHF model. The rats with confirmed CHF were then randomly allocated to six groups: sham group (Sham), model group (Model), low-dose YXT granule group (Low, 1.4 g/kg), medium-dose YXT granule group (Middle, 2.8 g/kg), high-dose YXT granule group (High, 5.6 g/kg), and trimetazidine group (TMZ, 0.01 g/kg). The Model group received an equivalent volume of distilled water, administered once daily. After 4 weeks of therapeutic intervention, rats were humanely sacrificed under anesthesia, allowing complete exposure of their thoracic and abdominal cavities. Various biological specimens, including serum, colonic tissue, myocardial tissue, and fecal content from the colon, were collected for analysis.

2.3 Cell culture and group treatment

A rat cardiomyocyte cell line, H9c2, obtained from Wuhan Procell Life Technology Co., Ltd., (Wuhan, China), was cultured in high-glucose Dulbecco's Modified Eagle Medium (DMEM, Cat No. PM150210, Procell) supplemented with 10% fetal bovine serum (FBS, Cat No. 164210-50, Procell) and 1% (v/v) penicillin/streptomycin (Cat No. PB180120, Procell) at 37°C in a 5% CO2 incubator. Twenty healthy adult male rats were randomly divided into two groups: the YXT group (5.6 g/kg/day) and the control group (equivalent saline), with gavage administration lasting 10 days. Two hours post-final gavage, rat serum was collected, and the supernatant was centrifuged and filtered through a 0.22 μ m microwell filter membrane. The serum was then refrigerated at 56°C for 30 min, followed by reheating in a 37°C constant temperature bath before experimentation. H9c2 cells

were cultured until reaching 70–80% confluence. Subsequently, the cells were randomly divided into the nine groups: CON group (10% FBS), LPS group (1 $\mu g/L$; Cat No. L2630-10MG, Sigma), YXT drug serum group (10%), Cholic acid (CA) group (100 $\mu g/mL$; Cat. No. HY-N0324, MCE), Deoxycholic Acid (DCA) group (150 $\mu g/mL$; Cat. No. HY-N0593, MCE), Chenodeoxycholic Acid (CDCA) group (150 $\mu g/mL$; Cat. No. HY-76847, MCE), Lithocholic Acid (LCA) group (30 $\mu g/mL$; Cat. No. HY-B0172, MCE), TGR5 inhibitor group (100 $\mu g/mL$ SBI-115; Cat. No. HY-111534, MCE), and TGR5 agonist group (100 $\mu g/mL$ INT-77; Cat. No. HY-15677, MCE). All groups, except for the CON group, were treated with 1 $\mu g/L$ LPS for 12 h. Afterward, each group was treated with respective drug concentrations for 24 h. Following treatment, cell pellets and supernatants were collected for further analysis.

2.4 Indicator detection and methods

2.4.1 Echocardiographic assessment of cardiac function

After a four-week treatment, rats were anesthetized with isoflurane (Cat. No. 22090401, Shenzhen Rayward Life Technology Co., Ltd., Shenzhen, China). Subsequently, left ventricular EF and FS were examined utilizing a high-resolution small animal echocardiography system (Feieno Technology Co., Ltd., Version: 6 LAB) to assess the subjects' cardiac function.

2.4.2 Histopathological analysis

After fixation in 10% paraformaldehyde, colon and cardiac tissues underwent dehydration followed by paraffin embedding. Sections were stained with hematoxylin and eosin (HE) and histological changes in colon and myocardial tissues were assessed under an optical microscope (Eclipse E100, Nikon, Japan).

2.4.3 16S rRNA gene sequencing

Bacterial genomic DNA was extracted from rat fecal samples using the cetyltrimethylammonium bromide (CTAB) method. The target sequence was amplified with 16S rRNA genespecific primers (5'-AGRGTTTGATYNTGGCTCAG-3' and 5'-TASGGHTACCTTGTTASGACTT-3'). The PCR product was purified using AMPure XT beads (Beckman Coulter Genomics, Danvers, MA, USA) and quantitatively assessed with Qubit (Invitrogen, USA). The purified PCR products were sequenced using an Agilent 2100 Bioanalyzer library quantification kit (Agilent, USA) and Illumina (KapaBiosciences, Woburn, MA, USA) to acquire the 16S rRNA gene sequences. Subsequently, the data underwent splicing and filtering for species diversity analysis and sequence alignment.

2.4.4 BA profiling

A 100 μL aliquot was mixed with a methanol solution (400 μL , Cat. No. CAEQ-4-000306-4000, CNW Technologies) and acetonitrile (Cat. No. CAEQ-4-000308-4000, CNW Technologies) in a 1:1 ratio. The resulting mixture was subjected to centrifugation at 12,000 rpm for 15 min at 4 °C. The supernatant was subsequently collected for further UHPLC-MS/MS analysis. A 1 mg/mL stock solution of the standard was prepared and subsequently diluted to generate a series of calibration solutions. For UHPLC-PRM-MS analysis, the target compounds underwent chromatographic

TABLE 1 Primer sequences for real-time quantitative PCR.

Target gene		Primer sequence(5′→3′)		
TGR5	Forward	CTATGGAATAGGAGCCATCAGGG		
	Reverse	GCAGGGAGAGGAAACAAAAGTTG		
GAPDH	Forward	GGCACAGTCAAGGCTGAGAATG		
	Reverse	ATGGTGGTGAAGACGCCAGTA		

separation utilizing a Vanquish UPLC system (Thermo Fisher Scientific) equipped with a Waters ACQUITY UPLC BEH C18 column (150 mm \times 2.1 mm, 1.7 μm , Waters). The mobile phase for liquid chromatography comprised a 5 mmol/L aqueous ammonium acetate solution (Phase A, catalog number CAEQ4-013465-0100, CNW Technologies) and acetonitrile (Phase B). The column compartment was maintained at 45°C and the sample tray at 4 °C, with a 1 μL injection volume. Mass spectrometric analysis was performed with an Orbitrap Exploris 120 high-resolution mass spectrometer operating in parallel reaction monitoring (PRM) mode.

2.4.5 Real-time quantitative PCR (RT-qPCR) analysis

Total RNA was extracted from rat myocardial tissue using an ultrapure RNA extraction kit. RNA purity and concentration were evaluated, and then reverse transcription was carried out to synthesize complementary DNA (cDNA). The PCR reaction was conducted in a 20 μL volume, beginning with an initial denaturation at 95 °C for 10 min, followed by 43 amplification cycles, each consisting of 10 s at 95 °C for denaturation, 10 s at 60 °C for primer annealing, and 10 s at 72 °C for extension. Gene expression levels were quantified using the $2^{-\Delta\Delta Ct}$ method, with GAPDH serving as the internal control. Primers were designed and synthesized by Hunan Accurate Biology, with sequences detailed in Table 1.

2.4.6 Western blot analysis

Cardiac tissues and cells were collected in EP tubes and lysed with RIPA buffer. After homogenization and a 30-minute incubation on ice, samples were centrifuged at 12,000 rpm for 10 min at 4 °C. Supernatants were collected for protein quantification using the BCA assay. Equal amounts of protein from each group were separated electrophoretically using a fast gel kit. The proteins were transferred onto PVDF membranes, and then blocked with a 5% milk solution for 2 h. Membranes were incubated overnight with TGR5 and GAPDH antibodies, followed by incubation with a secondary antibody at 37 °C for 2 h. Protein signals were analyzed using "Imedium" software. Immunoblot analysis was performed using the following antibodies: TGR5 (1: 1000, Abcam, ab72608), GAPDH (1: 1000, Servicebio, GB11002), and horseradish peroxidase-goat anti-rabbit (1:3000, Servicebio, GB23303).

2.4.7 ELISA assay of BNP, cAMP, IL-6, TNF- α , IL-1 β

Serum samples from rats and the supernatants of cultured cells were collected for analysis. The concentrations of serum cAMP, BNP and inflammatory cytokines interleukin-1 beta (IL-1 β), IL-6, and tumor necrosis factor-alpha (TNF- α) in both serum and supernatants were quantified using commercially available

ELISA assay kits: for cAMP (Cat No. A107988,Shanghai Fusheng Industrial Co., Ltd., China), BNP (Cat No. AF2943-A, Jiangsu Jingmei Biotechnology Co., Ltd., China), IL-1 β (Cat No. AF2923-A, Jiangsu Jingmei Biotechnology Co., Ltd., China), IL-6 (Cat No. AF3066-A, Jiangsu Jingmei Biotechnology Co., Ltd., China) and TNF- α (Cat No. AF3056-A, Jiangsu Jingmei Biotechnology Co., Ltd., China).

2.5 Statistical analysis

Data were statistically analyzed using one-way ANOVA or, for non-normally distributed data, the Kruskal-Wallis test, utilizing SPSS 26.0. The Spearman's Rank Correlation Coefficient method was employed to visualize the correlations among the data. A P-value of <0.05 was considered statistically significant, whereas P-value of <0.01 indicated high significance. Data distributions were visualized by generating histograms using GraphPad Prism 9.0.

3 Results

3.1 Chemical composition and stability of YXT

To clarify the mechanism through which YXT treats CHF, we analyzed the blood entry chemistry of YXT using UHPLC-QE/MS and identified 1049 blood entry chemistry components, including saponins, flavonoids, sterols, phenolic compounds, phenolic acids, terpenoids, and other related compounds, compounds such as 3-O-Acetyl-16alpha-hydroxytrametenolic acid, Alisol A, Alisol F, Foliosidine, Pachymic acid, Pygenic acid A and B, Formononetin, 29-hydroxypolyporenic acid C, Astragaloside IV, Kaempferol 7-O-glucoside, Ginsenoside Rg3, Tanshinone IIb, Rosmarinic acid, Ginsenoside Rg5, o-Xylene, Formononetin 7-(6"-malonylglucoside), Microtoenin B, and Cryptotanshinone, among others, are included (Figure 1 and Tables 2, 3).

3.2 YXT improves cardiac function in CHF rats

Electrocardiographic analysis revealed normal waveforms in healthy rats, whereas ligated rats exhibited significant ST-segment elevation and peaked T-waves, confirming successful coronary ligation and myocardial ischemia. The EF and FS value significantly decreased and the BNP level significantly increased in the Sham group (P < 0.01). After treatment, TMZ and YXT at all doses reduced serum BNP levels (P < 0.01), the EF value of High group, FS of TMZ and YXT at all doses increased (P < 0.01), (Figure 2).

3.3 YXT improves the pathological damage of heart tissue and colon in CHF rats

The histological results in both cardiac and colonic tissues are depicted in Figure 3. HE staining revealed that the cardiac

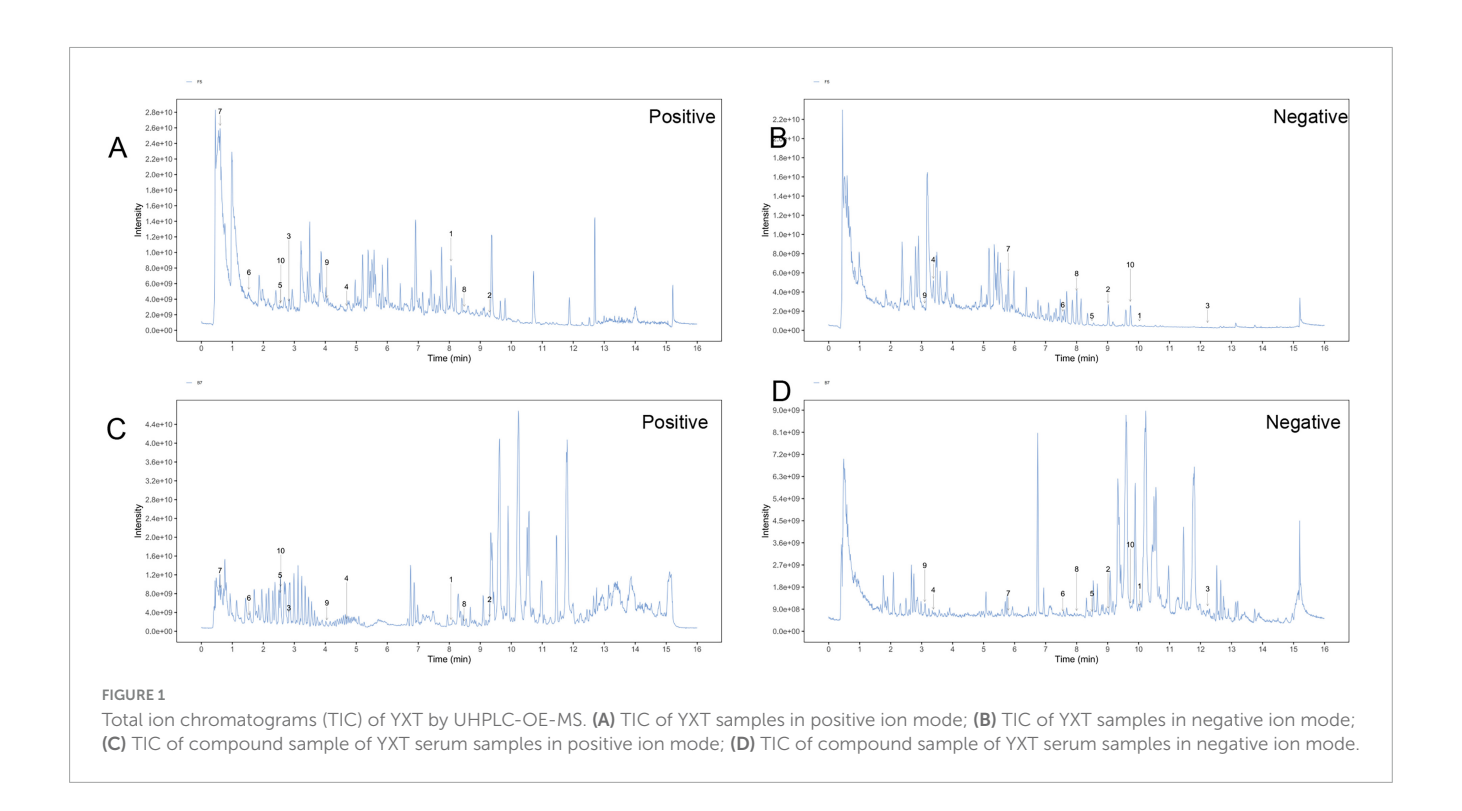
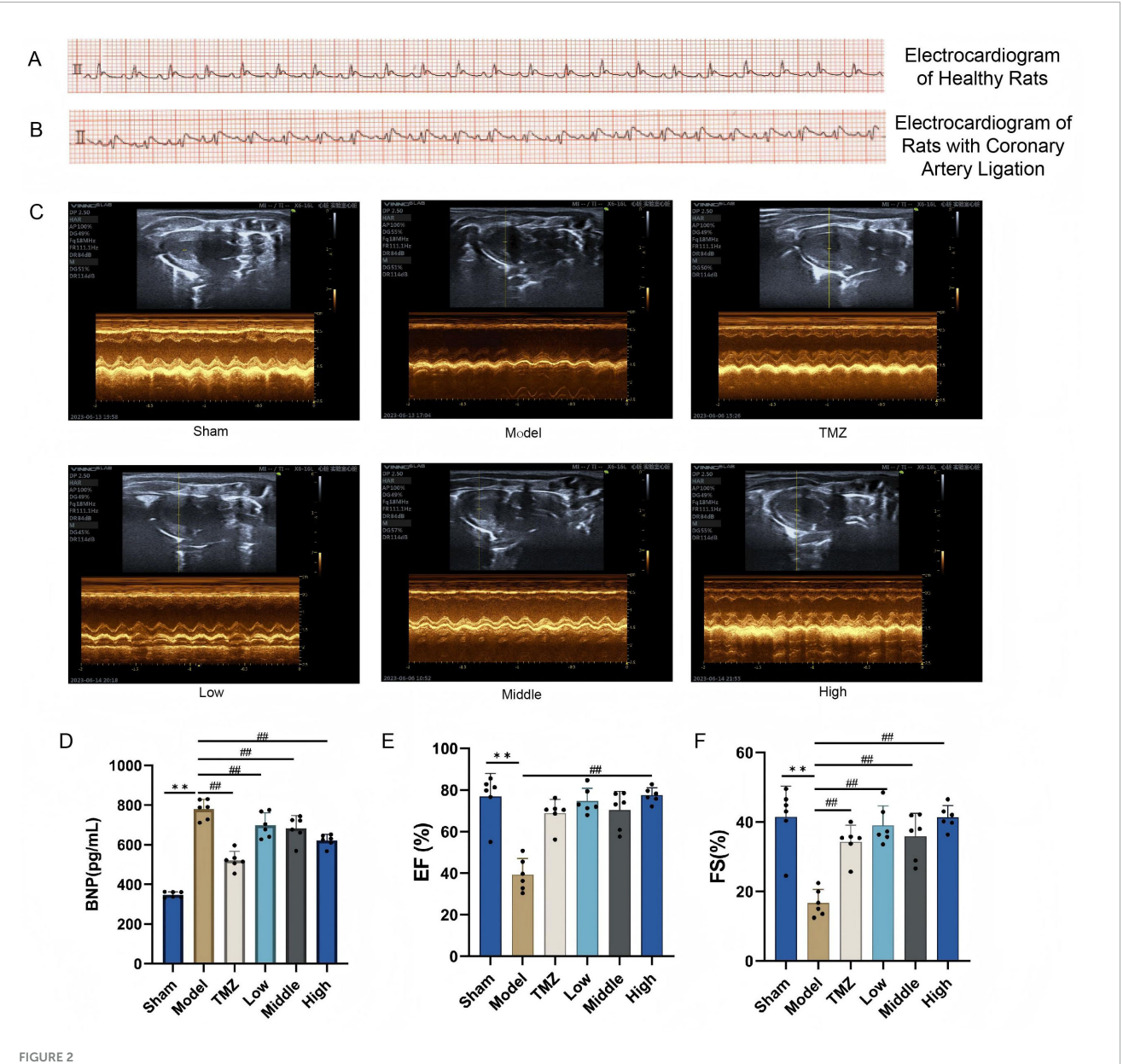


TABLE 2 Chemical composition list of YXT in positive ion mode.

ID	Name EN	Formula	mzmed	rtmed	Туре
1	Alisol F	C30H48O5	511.3406158	483.4705	Pos
2	Cryptotanshinone	C19H20O3	297.1483005	557.9945	Pos
3	Guanosine	C10H13N5O5	284.1000727	169.322	Pos
4	Salviamine B	C18H13NO3	292.0964186	281.054	Pos
5	Isorhamnetin	C16H12O7	317.0649346	152.402	Pos
6	Kaempferol 7-O-glucoside	C21H20O11	449.1075539	92.13285	Pos
7	p-Coumaric acid	С9Н8О3	165.0543267	36.27725	Pos
8	Tanshinone IIb	C19H18O4	311.1278585	508.9575	Pos
9	Formononetin 7-(6"-malonylglucoside)	C25H24O12	517.1336145	243.029	Pos
10	Methyl cinnamate	C10H10O2	163.0751635	153.482	Pos

TABLE 3 Chemical composition list of YXT in negative ion mode.

ID	Name EN	Formula	mzmed	rtmed	Туре
1	3-O-Acetyl-16alpha-hydroxytrametenolic acid	C32H50O5	513.3580238	601.897	Neg
2	Alisol A	C30H50O5	535.3641607	540.952	Neg
3	Pachymic acid	C33H52O5	527.3741541	733.7295	Neg
4	Formononetin	C16H12O4	267.0664777	202.63	Neg
5	29-Hydroxypolyporenic acid C	C31H46O5	497.3275221	509.751	Neg
6	Fargoside E	C42H66O14	793.4399862	453.367	Neg
7	Astragaloside IV	C41H68O14	829.4583253	347.675	Neg
8	Ginsenoside Rg3	C42H72O13	783.4894956	480.099	Neg
9	Rosmarinic acid	C18H16O8	359.0779182	185.834	Neg
10	Ginsenoside Rg5	C42H70O12	765.4783791	583.9125	Neg



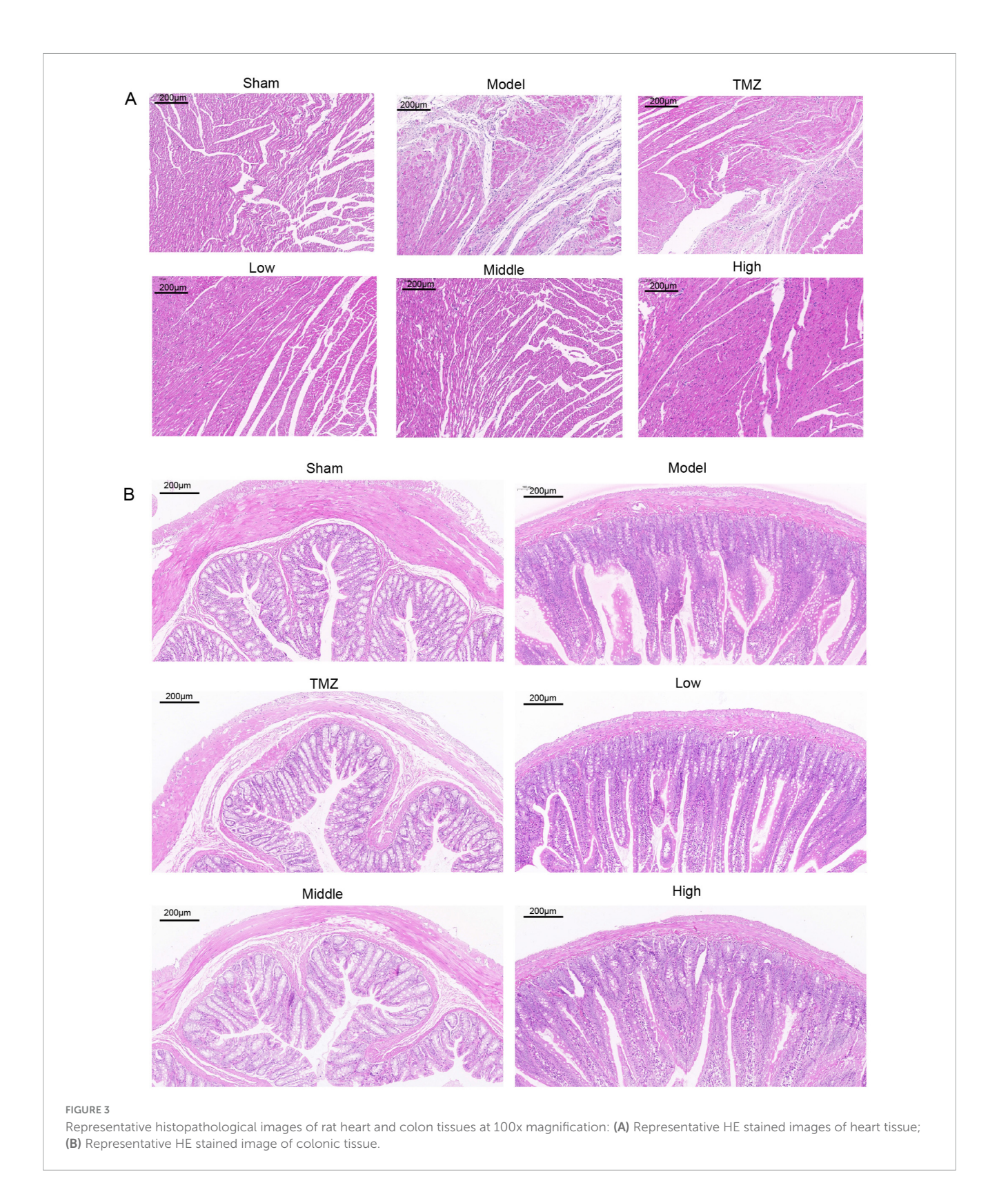
Cardiac ultrasound results and serum BNP levels in rats. (A) Electrocardiograms of healthy rats; (B) Coronary artery ligation-induced heart failure rats; (C) Quantitative evaluation of cardiac function based on short axis images of 2 D echocardiography; (D) Serum BNP levels; (E) EF was used to determine cardiac systolic function; (F) FS was used to determine cardiac systolic function. **P < 0.01, vs Sham; ##P < 0.01, vs Model; all values are expressed as the SD \pm mean.

tissue of the Sham group displayed a well-organized arrangement of cardiomyocytes without significant pathological changes. Conversely, the Model group exhibited substantial morphological alterations, such as distorted cells, edema, disorganized structure, and epicardial infiltration. Following treatment, the TMZ, Low, Middle, and High groups demonstrated varying degrees of improvement in cardiac tissue integrity compared with the Model group. Meanwhile, the colonic tissue of the Sham group displayed no significant inflammatory infiltration; goblet cells were regularly arranged, the number of glands remained unchanged, and the crypt structure was well-defined. Conversely, in the Model group, rats demonstrated a reduction in the number of goblet cells with disordered arrangement, marked inflammatory infiltration

in multiple regions, and an indistinct crypt structure. Following treatment, the pathological alterations in the colonic structure of the rats were mitigated, with the most pronounced improvements observed in the TMZ group and the Middle-dose YXT group.

3.4 YXT improves the gut microbiota disorder in CHF rats

The gut microbiome plays a critical role in the development and progression of CHF. Therefore, we analyzed 16S rRNA gene sequences from fecal samples of the colon to evaluate the structural changes in the gut microbial community. As



shown in Figures 4A–C, the correlation coefficient curve, species accumulation curve, and Shannon diversity index for all experimental groups exhibited a trend toward stabilization, reflecting a rich and uniform gut microbiota. Moreover, the stabilization of these metrics suggests that the sequencing depth was sufficient to accurately reflect the complexity and diversity

of the microbial communities under investigation. Figures 4D–F reveal a reduction in the Chao1 in the Model group compared with the Sham group. Figures 4G–K shows that inter-group distances exceeded intra-group distances, with a significant difference between the Model and Sham groups. After treatment, the distances between the TMZ, Low, Middle, High groups

and the Model were notably larger than within each group, especially in the Low group, where differences were statistically significant. However, these indices increased after TMZ and YXT treatments, with the Middle group showing the most significant improvement. Principal Coordinates Analysis (PCoA) and anosim analysis was conducted to assess beta diversity and revealed that distances within groups were smaller than those between groups. Additionally, the Model and Sham groups were clearly distinct, suggesting notable differences in microbiota diversity. Collectively, these findings indicate that YXT treatment may significantly improve gut microbiota diversity in CHF rats.

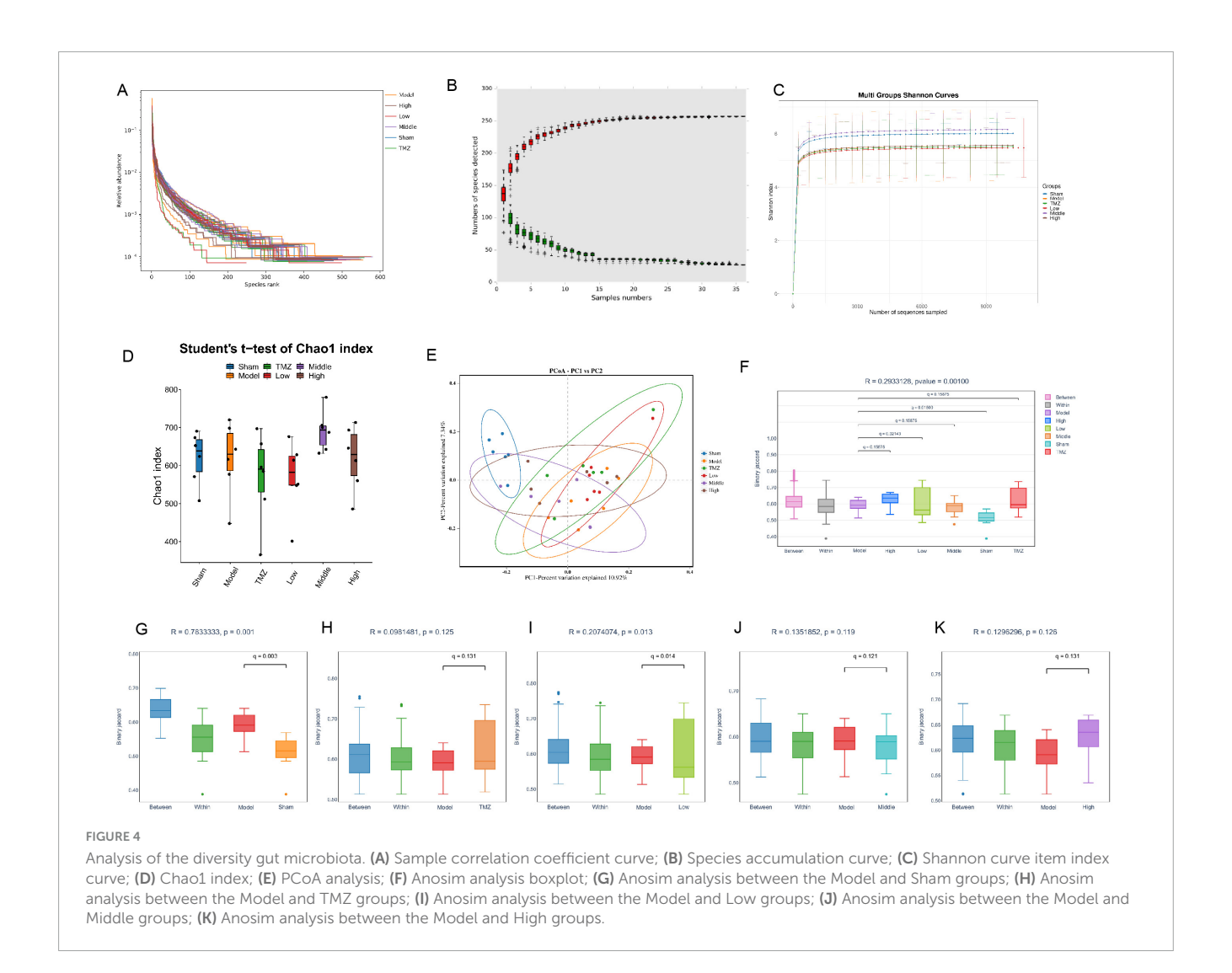
Relative to Sham group, the Model group showed a marked elevation abundances of Firmicutes, Desulfobacterota, Actinobacteriota, Patescibacteria, Verrucomicrobiota, Cyanobacteria at the phylum level. However, Bacteroidota, Proteobacteria, and Campylobacterota were depleted. The abundance of Firmicutes, Desulfobacterota, Actinobacteriota, Patescibacteria, Verrucomicrobiota, Cyanobacteria decreased, whereas that of Bacteroidota and Campylobacterota bacteria increased in the TMZ, Low, Middle, and High groups versus the Model group (Figure 5A). At the family level, the Model group displayed higher relative abundances of Lactobacillaceae, Lachnospiraceae, Ruminococcaceae, and an uncultured rum bacterium compared with the Sham group. Conversely, the relative abundances of Erysipelotrichaceae, Muribaculaceae, Oscillospiraceae, unclassified Clostridia UCG-014, Prevotellaceae, and the [Eubacterium] coprostanoligenes group were diminished in the Model group compared with the Sham group. The relative abundances of Lactobacillaceae, Lachnospiraceae, and Ruminococcaceae were decreased, while those of Erysipelotrichaceae, Muribaculaceae, Oscillospiraceae, Prevotellaceae, and the [Eubacterium] coprostanoligenes group were augmented in the TMZ, Low, Middle, and High groups compared with the Model group. Additionally, the relative abundance of unclassified Clostridia UCG-014 was elevated in the TMZ, Low, and Middle groups (Figure 5B). At the genus level, the Model group showed increased abundances of Lactobacillus, an unclassified rum bacterium, Lachnospiraceae_NK4A136_group, and Ligilactobacillus compared with the Sham group. Conversely, the abundance ratios of unclassified Muribaculaceae, Dubosiella, unclassified Clostridia_UCG_014, Allobaculum, unclassified [Eubacterium]_coprostanoligenes_group, and Alloprevotella were reduced in the Model group compared with the Sham group. The abundance proportions of Lactobacillus, Lachnospiraceae_NK4A136_group, and Ligilactobacillus decreased, whereas the abundance ratios of unclassified Clostridia_UCG_014, unclassified Muribaculaceae, Dubosiella, and unclassified [Eubacterium]_coprostanoligenes_group increased in the TMZ, Low, Middle, and High groups compared with the Model group (Figure 5C). At the species level, it was found that the abundances of uncultured rum bacterium and unclassified_Lachnospiraceae_NK4A136_group were significantly higher, while the abundance ratios of unclassified_Muribaculaceae, unclassified_Dubosiella, Lactobacillus_johnsonii, unclassified_ Clostridia_UCG_014, unclassified_Allobaculum, and unclassified_ [Eubacterium]coprostanoligenes_group were notably lower in the Model group than in the Sham group. In addition, the abundance ratios of unclassified_Lachnospiraceae_NK4A136_group, Lacto bacillus_murinus, and Lactobacillus_acidophilus were decreased, whereas the proportions of unclassified_Muribaculaceae, unclassified_Dubosiella, and unclassified[Eubacterium]_coprostanoligenes_group were increased in the TMZ, Low, Middle, and High groups compared with the Model group (Figures 5D, E).

3.5 YXT improves serum BA levels in CHF rats

The gut microbiota significantly influences BA metabolism through BA hydrolysis enzymes, affecting BA biosynthesis and their corresponding signaling pathways. Hence, we investigated the relationship between gut microbiota at the genus level and BA to elucidate the intricate interactions between microbial populations and BA. In comparison to the Sham group, the Model group demonstrated a significant reduction in serum levels of various BA, including CDCA, CA, DCA, LCA, ursodeoxycholic acid (UDCA), ursocholic acid (UCA), allocholic acid (ACA), hyodeoxycholic acid (HDCA), 3-epideoxycholic acid (3-EDCA), 6-ketolithocholic acid (6-KLCA), isohyodeoxycholic acid (IsoHDCA), and α-muricholic acid (α -MCA), with statistical significance (P < 0.05 or P < 0.01). Subsequent to treatment, an elevation in these BA levels was observed across the TMZ, Low-, Middle-, and High-dose Yixintai groups. Notably, the High-dose group exhibited statistically significant increases in CDCA, CA, DCA, UDCA, HDCA, 3-EDCA, and 6-KLCA (P < 0.05 or P < 0.01). Additionally, the Low- and Middle-dose groups showed significant upregulation of CA (P < 0.05 or P < 0.01). The results are illustrated in the heatmap shown in Figure 6. It was found that certain bacteria, such as Allobaculum? Alloprevotella, Dubosiella, unclassified_ [Eubacterium]_coprostanoligenes_group, Clostridia_UCG_014, unclassified_Muribaculaceae and uncultured_rumen_bacterium were positively correlated with nearly all BA. However, Lachnospiraceae_NK4A136_group, Lactobacillus and Ligilactobacillus exhibited were negatively correlated with most BA.

3.6 YXT improves the expression of TGR5 and suppresses the cardiac inflammatory response

As depicted in Figure 7, mRNA and protein expression levels of TGR5 were notably reduced in the Model group when compared with the Sham group (P < 0.01), post-treatment by TMZ and YXT, the mRNA and protein expression levels of TGR5 were markedly elevated relative to the Model group (P < 0.05 or P < 0.01), the serum concentrations of cAMP were lower in the Model group (P < 0.05), after treatment, the serum cAMP levels were significantly elevated in the TMZ, Middle and High groups when compared to the Model group (P < 0.01). The serum concentrations of, IL-1 β , IL-6, and TNF- α were notably higher in the Model group. However, after treatment, these serum levels were significantly reduced in the TMZ, Low, Middle, and High groups when compared to the Model group. These results suggest that YXT can inhibit the inflammatory response in heart failure rats by activating TGR5 expression.

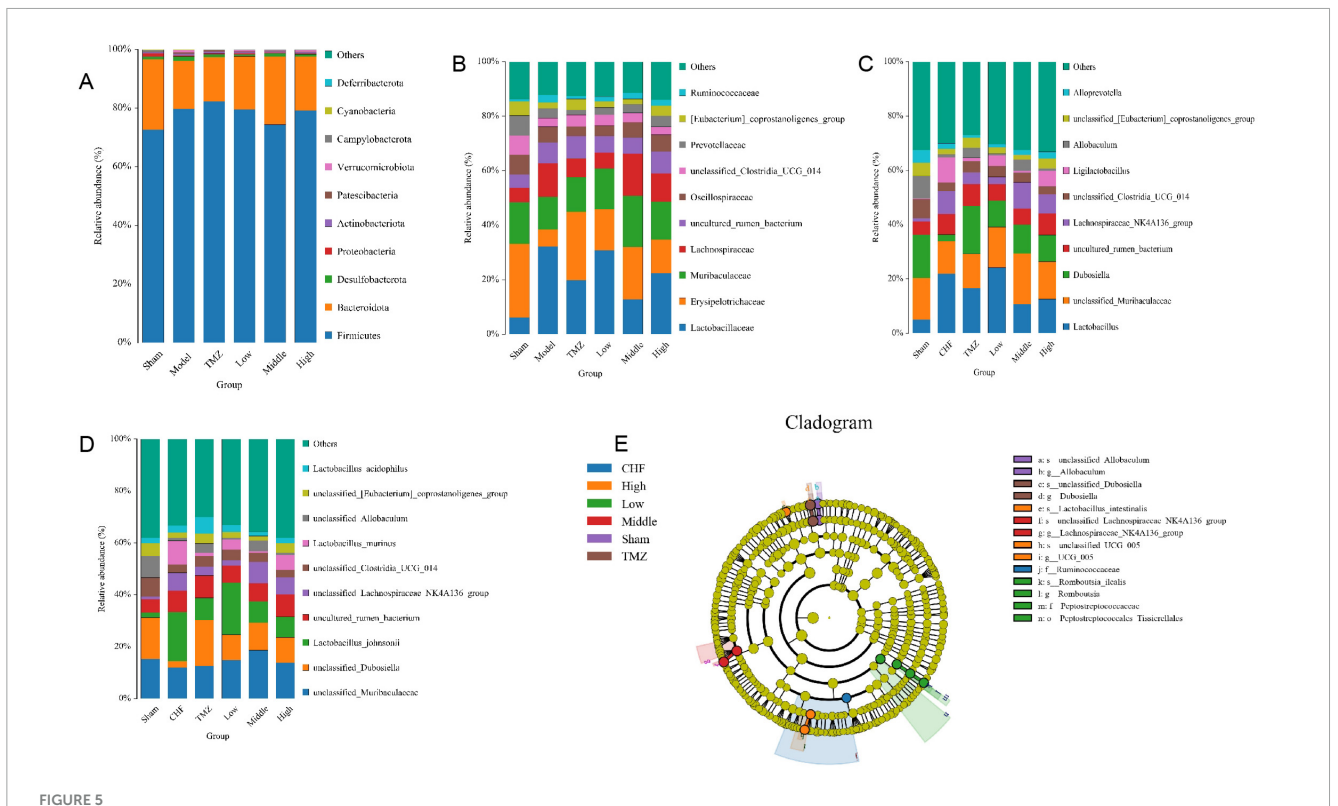


3.7 YXT drug-containing serum promotes the expression of TGR5 in H9c2 cells and improves the inflammatory damage of H9c2 cells

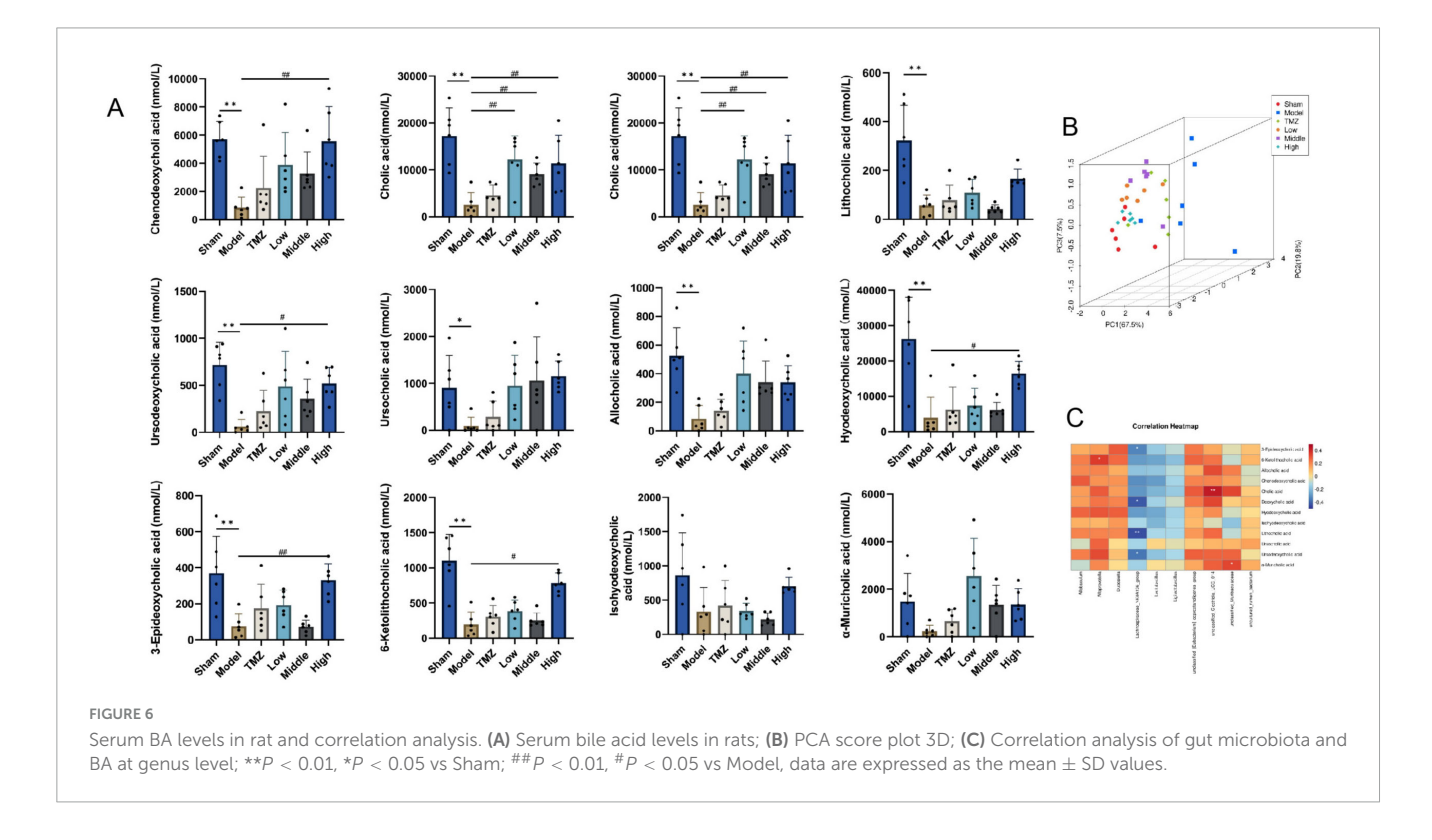
As illustrated in Figure 8, cell viability was significantly inhibited after LPS intervention in H9c2 cardiomyocytes compared with the CON group (P < 0.01). Compared with the LPS group, the cell viability was markedly increased after treatment with YXT containing serum, CA, DCA, and LCA (P < 0.01). The mRNA levels of TGR5 in H9c2 cells were elevated in the CDCA, CA, DCA, and LCA groups compared with the LPS group (P < 0.05or P < 0.01). Compared with the CON group, the LPS group exhibited a downward trend in the TGR5 protein levels (P < 0.01), the protein levels of TGR5 in H9c2 cells from the YXT, CDCA, CA, and INT-777 groups were increased (P < 0.05 or P < 0.01). Compared with the CON group, the supernatant levels of IL-6, IL- 1β and TNF- α in H9c2 cells were significantly higher in the LPS group (P < 0.01), treatment with YXT, CDCA, CA, DCA, LCA, and INT-777 significantly reduced IL-6, IL-1 β and TNF- α levels in H9c2 cell supernatants (P < 0.05 or P < 0.01). The results suggest that the activation of TGR5 plays a mediating role in the anti-inflammatory effects of Yixintai on H9c2 cells, as demonstrated by the observed reduction in inflammatory injury following treatment with serum containing the drug.

4 Discussion

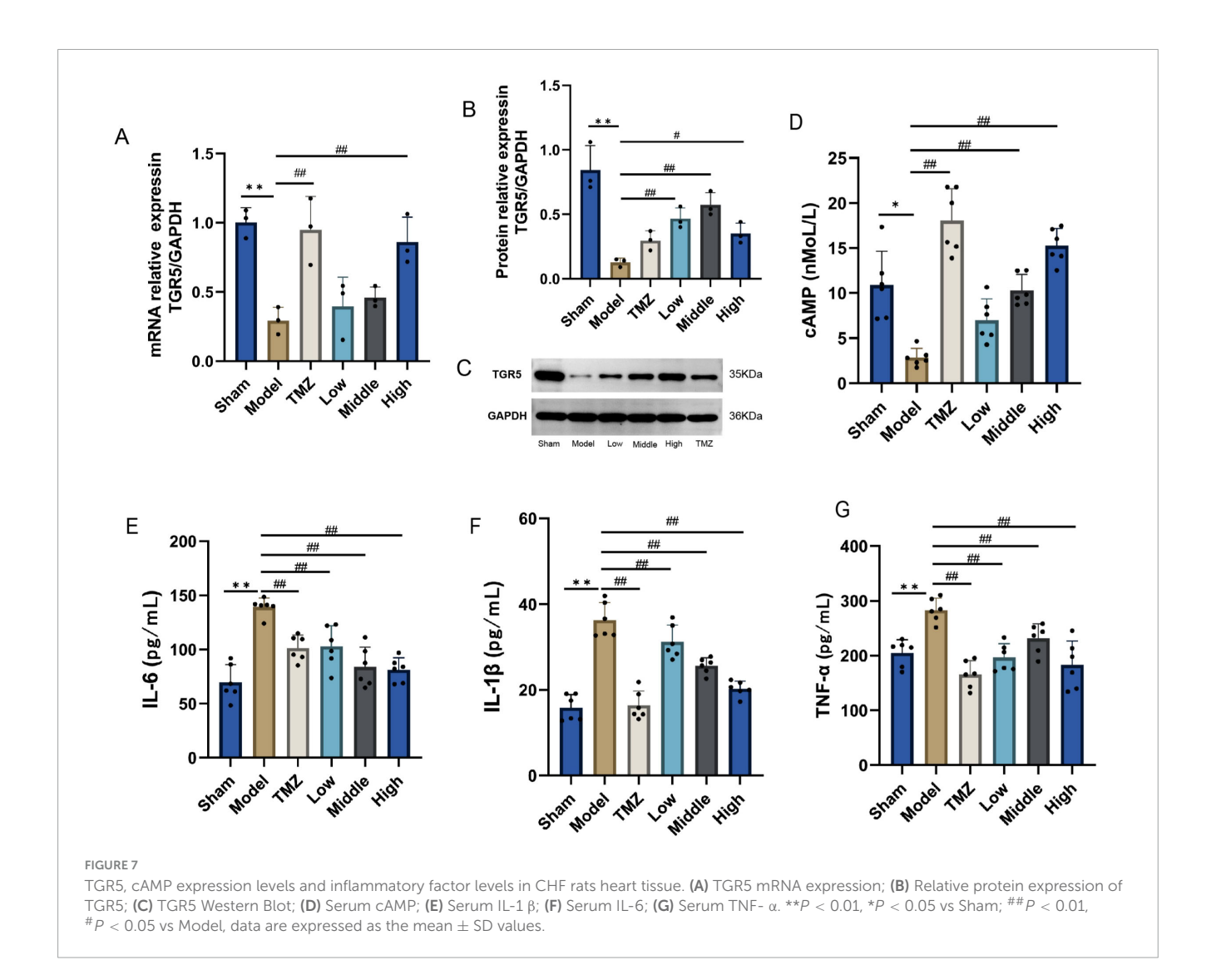
Chronic heart failure (CHF) is a complex clinical condition influenced by multiple factors such as congenital heart defects, diabetes, obesity, smoking, myocarditis, cardiomyopathy, hypertension, and coronary artery disease. Therefore, CHF should be viewed as a multifaceted syndrome rather than a singular disease (Baman and Ahmad, 2020). The gut microbiota, as the largest microbial ecosystem in the human body, plays a crucial role in regulating a range of physiological functions. Maintaining the dynamic balance of this microbiota is crucial for human health, the formation of a mucosal immune barrier, and the prevention of pathogen colonization (Branchereau et al., 2019). During CHF, reduced cardiac EF and output cause both systemic and gastrointestinal congestion, leading to ischemia, hypoxia, and edema in the intestinal mucosa, thereby compromising the intestinal barrier and disrupting microcirculation. Concurrently, the equilibrium of gut bacteria is disrupted, promoting bacterial



Analysis of the abundance of gut microbiota. (A) Gut microbiota relative abundance at phylum level; (B) Gut microbiota relative abundance at family level; (C) Gut microbiota relative abundance at genus level; (D) Gut microbiota relative abundance at species level; (E) LEfSe evolutionary branching diagram.



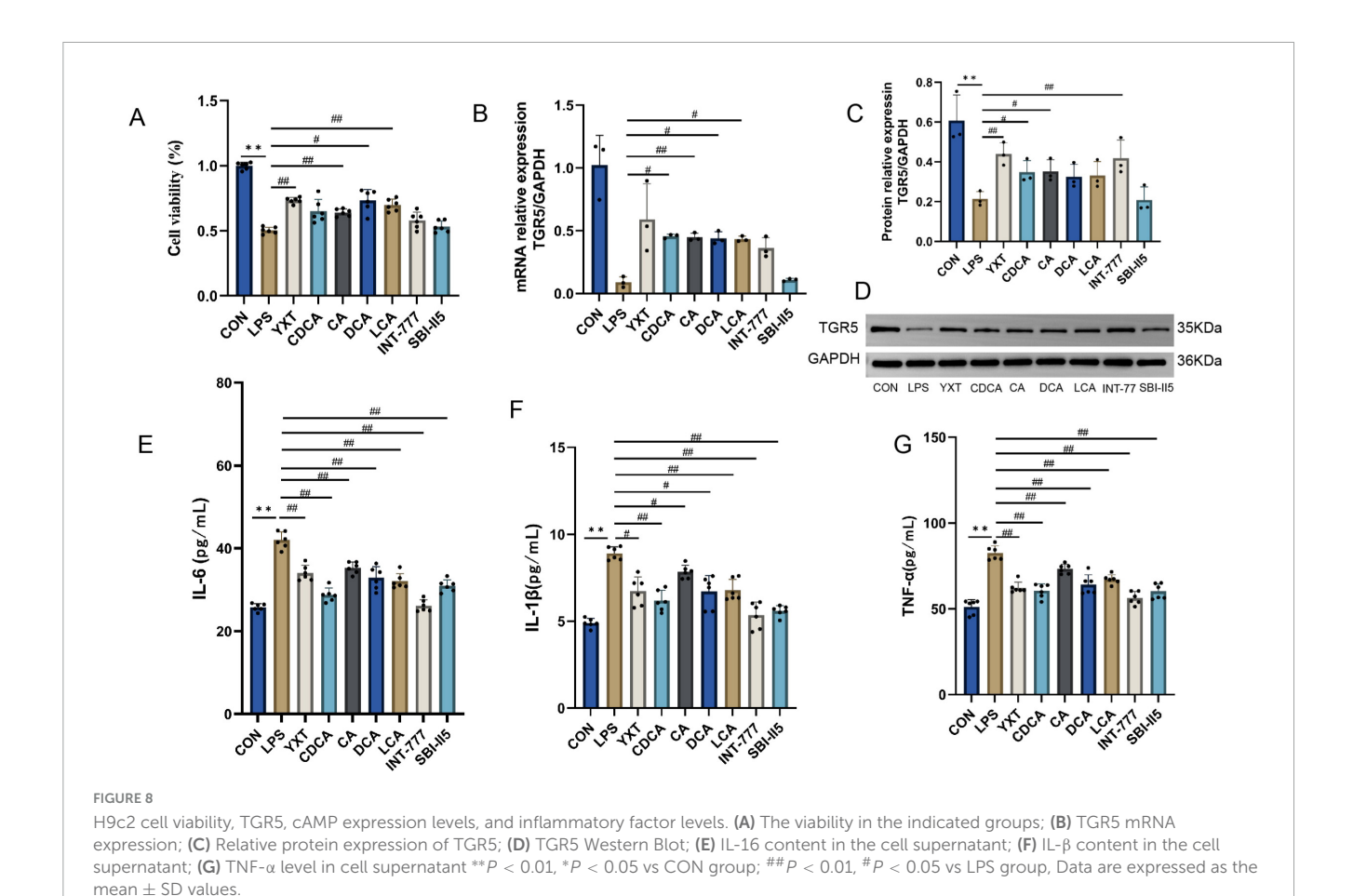
translocation, endotoxemia, and the secretion of inflammatory mediators. These processes initiate systemic inflammation, impair vascular endothelial function, impede blood flow and nutrient delivery, and ultimately result in multi-organ dysfunction, thereby exacerbating the severity of CHF (Formiga et al., 2019; Jain et al., 2024; Yang et al., 2024). The present study demonstrated



that CHF rats showed substantial infiltration of inflammatory cells and disruption of intestinal mucosal integrity, suggesting an inflammatory response. Elevated serum levels of IL-1 β , IL-6, TNF- α , and BNP, along with reduced EF and impaired cardiac function, corroborated these findings. Conversely, rats treated with YXT showed a significant reduction in serum inflammatory markers, enhanced cardiac function, and alleviated pathological changes in both cardiac and colonic tissues. These findings indicate that YXT effectively alleviates CHF by reducing the inflammatory response.

Patients with CHF exhibited reduced gut microbiota diversity, increased abundance of harmful bacteria like *Shigella*, *Campylobacter*, *Salmonella*, *Yersinia*, and various *Candida* species. In contrast, they have lower number of beneficial bacteria, such as *Bifidobacterium* and *Lactobacillus* (Pasini et al., 2016). The severity of CHF is influenced by certain pathogens, with *Shigella*, *Campylobacter*, and *Candida*, considered as important microbiota affecting the prognosis (Yuzefpolskaya et al., 2020). Research suggests that disruption of gut microbiota may trigger chronic inflammation and immune dysfunction, potentially aggravating HF by lowering ejection fraction (Madan and Mehra, 2020). In this study, we found that rats with CHF exhibited reduced

microbial diversity. However, the YXT treatment restored the normal diversity of gut microbiota, supporting the notion that YXT can enhance cardiac function in CHF rats by rebalancing gut microbiota (Cui et al., 2018). Compared to the Sham group, the Model group exhibited an elevated Firmicutes abundance but a reduced Bacteroidota level. YXT administration significantly reversed these microbial shifts, lowering Firmicutes and enhancing Bacteroidota populations. This observation aligns with prior reports by Li et al. (2021); Zhang Q. L. et al. (2023) on gut microbiota modulation. In the study undertaken by Oliphant et al. (2021), Bacteroides was an important constituent of the microbiota's bacterial community. Furthermore, studies have demonstrated that Bacteroidota plays a pivotal role in generating health-promoting metabolites and modulating host immune responses. Furthermore, Zhang et al. (2020) demonstrated that Desulfobacterota contributes to intestinal inflammation, suggesting that fluctuations in their abundance were associated with LPS levels. Recent studies have identified specific microbiota associated with systemic inflammation. For instance, Liu et al. (2022) demonstrated a direct link between Actinobacteria and inflammatory processes, suggesting that elevated abundance of Actinobacteria may trigger an inflammatory cascade. Similarly, Drapkina et al. (2022) and her

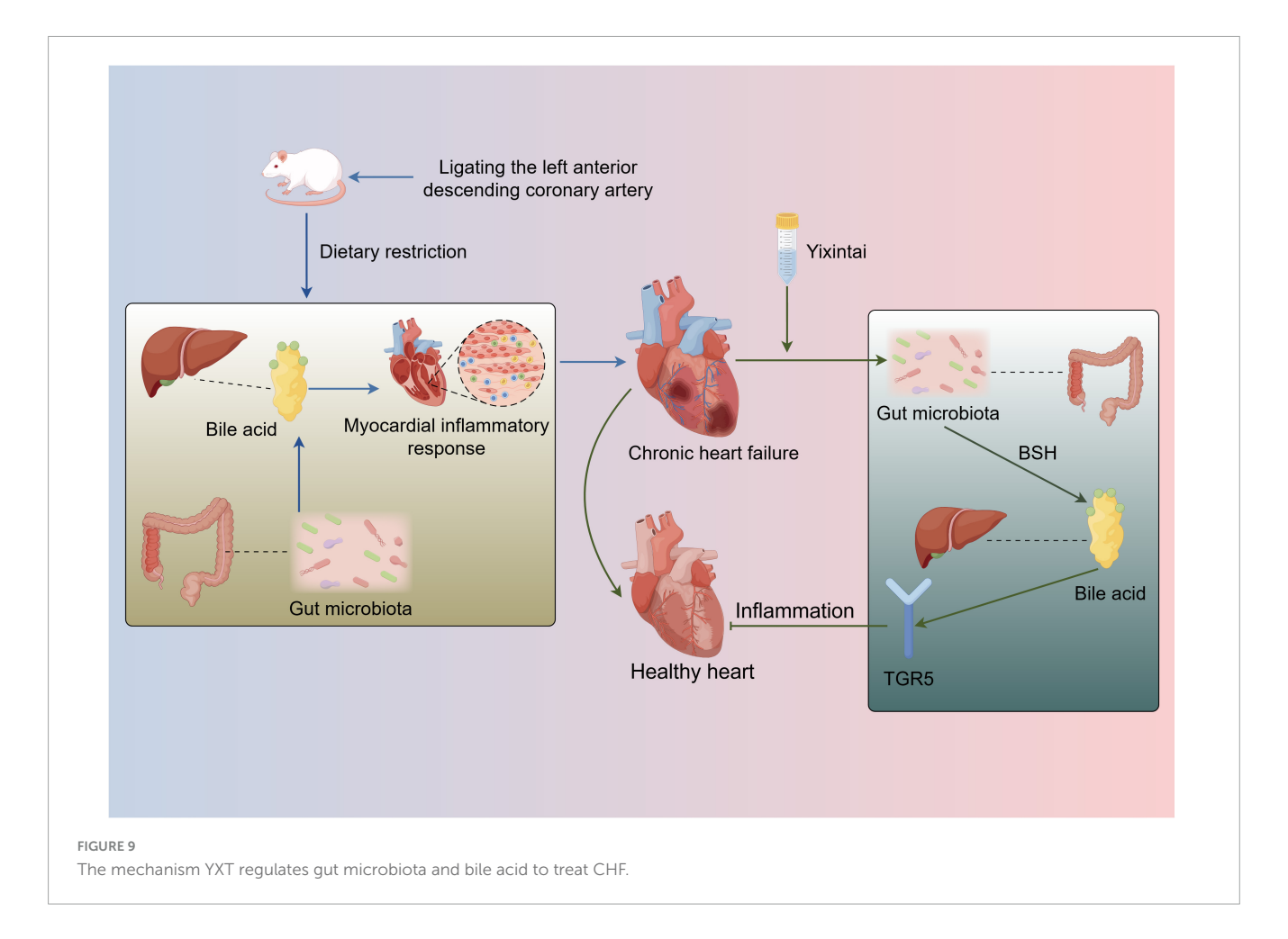


team reported that HF patients with reduced ejection fraction had elevated levels of *Lactobacillaceae* levels, which correlated with a more pronounced systemic inflammatory response. Elsewhere, Li et al. (2024). postulated that *Lachnospiraceae* could be a pathogenic factor, exacerbating the occurrence of inflammatory reactions. In this study, it was observed that rats with CHF exhibited higher abundances of *Desulfobacterota*, *Actinobacteriota*, *Lactobacillaceae*, and *Lachnospiraceae*. Following treatment with YXT, a notable reduction in the abundance of these specific microbiota was observed. This observation implies that YXT might contribute to alleviate the abundance of pathogenic bacteria in rats suffering from CHF.

Gut microbiota are important regulators of the cardiovascular health, with studies showing that compromised intestinal barrier will lead to bacterial translocation, causing activation of inflammatory and immune pathways. These mechanisms are implicated in the synthesis of various metabolites, including BA, SCFAs, TMAO, and other microbial byproducts. BA improve nutrient uptake in the intestines, regulating lipid and energy metabolism, and sustaining intestinal balance. Emerging evidence show that alterations in BA metabolic pathways may provoke inflammatory responses, thereby increasing the risk of developing CHF (Zhang S. et al., 2023). A prospective cohort study by Mayerhofer et al. reported that the BA levels were reduced in patients with CHF (Mayerhofer et al., 2017). Moreover, the study revealed that the serum BA levels in rats with CHF were decreased, but restored following treatment. Other investigations have shown

that Actinobacteria and Proteobacteria are involved in modulating the activity of BA, including chenodeoxycholic acid, cholic acid, deoxycholic acid, and lithocholic acid, which are essential for maintaining BA balance. Through receptor-mediated mechanisms, BA not only shape the gut microbiota but also orchestrate host metabolic and inflammatory processes (Komorniak et al., 2024). Herein, the Pearson's correlation analysis demonstrated a strong correlation between the abundance of specific gut microbiota, including [Eubacterium]_coprostanoligenes_group, Allobaculum, Alloprevotella, Clostridia_UCG_014, Dubosiella, uncultured_rumen_bacterium, and Muribaculaceae, and bile acid (BA) levels. This suggests that these microbial communities may increase the production of BA by modulating the activity of bile salt hydrolase (BSH). Therefore, YXT may regulate abundance of [Eubacterium]_coprostanoligenes_group, Allobaculum, Alloprevotella, Clostridia_UCG_014, Dubosiella, uncultured_rumen_bacterium and Muribaculaceae to augment BA metabolism and mitigate the inflammatory response associated with CHF.

Following their synthesis in the liver, BA are transported to the intestine where they act as molecular signals regulating cardiovascular function. TGR5, a widely researched membrane-bound G protein-coupled receptor, is expressed in multiple tissues throughout the body (Wahlström et al., 2016; Winston and Theriot, 2020; Perino et al., 2021). Prior investigations show that BA activate the TGR5 receptor to improve the function of cardiomyocytes, enhancing diastolic function, reducing inflammation in HF, and



stimulating the restoration of intestinal barrier (Liu et al., 2013; Zuo et al., 2015; Hanafi et al., 2018). Moreover, experimental evidence indicates that BA, functioning as TGR5 agonists, can protect murine myocardium, improving the heart's ability to respond to physiological, muscular, and hemodynamic stress. Considering that TGR5 participates in myocardial adaptability, its activation may be an attractive approach to treat HF (Eblimit et al., 2018). Moreover, disturbances in the gut microbiome and BA have been associated with the development of HF. BA activates the TGR5, thereby inhibiting inflammatory responses. This mechanism highlights the role of BA in immune regulation (Chen et al., 2020; Hu et al., 2021). In rats with CHF, TGR5 and cAMP expression levels were decreased, while serum levels of IL-1β, IL-6, and TNF-α were markedly increased. Interestingly, YXT treatment restored TGR5 and cAMP levels in cardiac tissues and reduced serum concentrations of IL-1β, IL-6, and TNF-α. These results suggest that YXT upregulates TGR5 expression in the heart to mitigate the inflammatory response in CHF rats. In vitro experiments showed that YXT-containing serum, combined with LCA, DCA, CDCA, CA, and the TGR5 agonist INT-777, alleviated LPS-induced damage in H9c2 cells. This treatment stimulated TGR5 and cAMP expression, suppressed inflammatory response and improved cardiomyocyte survival. Collectively, these findings indicate that the YXT's protective effects against LPS-induced H9c2 cardiomyocyte injury model were mediated by the interaction of BA with the TGR5 signaling pathway.

In conclusion, this study illustrates that YXT ameliorates gut microbiota dysbiosis in rats with CHF, subsequently modulating serum BA levels and activating the BA receptor TGR5 to suppress inflammatory responses, thereby achieving therapeutic effects against CHF. Nonetheless, several limitations must be acknowledged. While differential microbial taxa and BA levels were identified, further research is necessary to comprehensively elucidate the underlying mechanisms, future studies should investigate these findings in greater depth (Figure 9).

Data availability statement

The original contributions presented in the study are publicly available. This data can be found here: https://www.ncbi.nlm.nih.gov/bioproject/PRJNA1344468.

Ethics statement

The animal study was approved by the Institutional Animal Care and Use Committee (IACUC) of Hunan University of Chinese Medicine. The study was conducted in accordance with the local legislation and institutional requirements.

Author contributions

MS: Data curation, Formal analysis, Software, Writing – original draft. HY: Data curation, Software, Writing – original draft. CL: Formal analysis, Software, Writing – original draft. JW: Investigation, Writing – review & editing. ZW: Formal analysis, Software, Writing – original draft. AH: Data curation, Writing – original draft. QZ: Data curation, Writing – original draft. YL: Funding acquisition, Methodology, Resources, Writing – review & editing. ZG: Conceptualization, Funding acquisition, Methodology, Supervision, Writing – review & editing.

Funding

The author(s) declare that financial support was received for the research and/or publication of this article. This work was supported by the National Natural Science Foundation of China (82174343, 82405372); Key Research and Development Program of Hunan Province of China (2022SK2012); The Postdoctoral Fellowship Program of CPSF (GZC20252636); The China Postdoctoral Science Foundation (2025M773968, 2025T181082).

Acknowledgments

The Figure 9 was created by Figdraw.

References

Baman, J. R., and Ahmad, F. S. (2020). Heart failure. *JAMA* 324:1015. doi: 10.1001/jama.2020.13310

Bonfioli, G. B., Rodella, L., Metra, M., and Vizzardi, E. (2025). GLP-1 receptor agonists as promising anti-inflammatory agents in heart failure with preserved ejection fraction. *Heart Fail. Rev.* 30, 131–136. doi: 10.1007/s10741-024-10450-6

Branchereau, M., Burcelin, R., and Heymes, C. (2019). The gut microbiome and heart failure: A better gut for a better heart. *Rev. Endocr. Metab. Disord.* 20, 407–414. doi: 10.1007/s11154-019-09519-7

Chen, W., Wei, Y., Xiong, A., Li, Y., Guan, H., Wang, Q., et al. (2020). Comprehensive analysis of serum and fecal bile acid profiles and interaction with gut microbiota in primary biliary cholangitis. *Clin. Rev. Allergy Immunol.* 58, 25–38. doi: 10.1007/s12016-019-08731-2

Cui, X., Ye, L., Li, J., Jin, L., Wang, W., Li, S., et al. (2018). Metagenomic and metabolomic analyses unveil dysbiosis of gut microbiota in chronic heart failure patients. *Sci. Rep.* 8:635. doi: 10.1038/s41598-017-18756-2

Drapkina, O. M., Ashniev, G. A., Zlobovskaya, O. A., Yafarova, A. A., Dementeva, E. V., Kaburova, A. N., et al. (2022). Diversities in the gut microbial patterns in patients with atherosclerotic cardiovascular diseases and certain heart failure phenotypes. *Biomedicines* 10:2762. doi: 10.3390/biomedicines10112762

Eblimit, Z., Thevananther, S., Karpen, S. J., Taegtmeyer, H., Moore, D. D., Adorini, L., et al. (2018). TGR5 activation induces cytoprotective changes in the heart and improves myocardial adaptability to physiologic, inotropic, and pressure-induced stress in mice. *Cardiovasc. Ther.* 36:e12462. doi: 10.1111/1755-5922. 12462

Formiga, F., Ferreira Teles, C. I., and Chivite, D. (2019). Impact of intestinal microbiota in patients with heart failure: A systematic review. *Med. Clin.* 153, 402–409. doi: 10.1016/j.medcli.2019.06.006

Hanafi, N. I., Mohamed, A. S., Sheikh Abdul, Kadir, S. H., and Othman, M. (2018). Overview of bile acids signaling and perspective on the signal of ursodeoxycholic acid, the most hydrophilic bile acid, in the heart. *Biomolecules* 8:159. doi: 10.3390/biom8040159

Conflict of interest

The authors declare that the research was conducted in the absence of any commercial or financial relationships that could be construed as a potential conflict of interest.

Generative AI statement

The authors declare that no Generative AI was used in the creation of this manuscript.

Any alternative text (alt text) provided alongside figures in this article has been generated by Frontiers with the support of artificial intelligence and reasonable efforts have been made to ensure accuracy, including review by the authors wherever possible. If you identify any issues, please contact us.

Publisher's note

All claims expressed in this article are solely those of the authors and do not necessarily represent those of their affiliated organizations, or those of the publisher, the editors and the reviewers. Any product that may be evaluated in this article, or claim that may be made by its manufacturer, is not guaranteed or endorsed by the publisher.

Hu, J., Wang, C., Huang, X., Yi, S., Pan, S., Zhang, Y., et al. (2021). Gut microbiota-mediated secondary bile acids regulate dendritic cells to attenuate autoimmune uveitis through TGR5 signaling. *Cell Rep.* 36:109726. doi: 10.1016/j.celrep.2021.109726

Jain, H., Marsool, M., Goyal, A., Sulaiman, S. A., Fatima, L., Idrees, M., et al. (2024). Unveiling the relationship between gut microbiota and heart failure: Recent understandings and insights. *Curr. Probl. Cardiol.* 49:102179. doi: 10.1016/j.cpcardiol. 2023.102179

Khan, M. S., Shahid, I., Bennis, A., Rakisheva, A., Metra, M., and Butler, J. (2024). Global epidemiology of heart failure. *Nat. Rev. Cardiol.* 21, 717–734. doi: 10.1038/s41569-024-01046-6

Komorniak, N., Pawlus, J., Gaweł, K., Hawryłkowicz, V., and Stachowska, E. (2024). Cholelithiasis, gut microbiota and bile acids after bariatric surgery-can cholelithiasis be prevented by modulating the microbiota? A literature review. *Nutrients* 16:2551. doi: 10.3390/nu16152551

Li, C., Deng, L., Pu, M., Ye, X., and Lu, Q. (2024). Coptisine alleviates colitis through modulating gut microbiota and inhibiting TXNIP/NLRP3 inflammasome. *J. Ethnopharmacol.* 335:118680. doi: 10.1016/j.jep.2024.118680

Li, L., Zhong, S. J., Hu, S. Y., Cheng, B., Qiu, H., and Hu, Z. X. (2021). Changes of gut microbiome composition and metabolites associated with hypertensive heart failure rats. *BMC Microbiol.* 21:141. doi: 10.1186/s12866-021-02202-5

Liu, B., Ding, Z., Xiong, J., Heng, X., Wang, H., and Chu, W. (2022). Gut microbiota and inflammatory cytokine changes in patients with ankylosing spondylitis. *Biomed. Res. Int.* 2022:1005111. doi: 10.1155/2022/1005111

Liu, X., Fassett, J., Wei, Y., and Chen, Y. (2013). Regulation of DDAH1 as a potential therapeutic target for treating cardiovascular diseases. *Evid. Based Compl. Alternat. Med.* 2013:619207. doi: 10.1155/2013/619207

Luqman, A., Hassan, A., Ullah, M., Naseem, S., Ullah, M., Zhang, L., et al. (2024). Role of the intestinal microbiome and its therapeutic intervention in cardiovascular disorder. *Front. Immunol.* 15:1321395. doi: 10.3389/fimmu.2024.1321395

Madan, S., and Mehra, M. R. (2020). Gut dysbiosis and heart failure: Navigating the universe within. Eur. J. Heart Fail. 22, 629–637. doi: 10.1002/ejhf.1792

Mayerhofer, C., Ueland, T., Broch, K., Vincent, R. P., Cross, G. F., Dahl, C. P., et al. (2017). Increased secondary/primary bile acid ratio in chronic heart failure. *J. Card. Fail.* 23, 666–671. doi: 10.1016/j.cardfail.2017.06.007

Nagatomo, Y., and Tang, W. H. (2015). Intersections between microbiome and heart failure: Revisiting the gut hypothesis. *J. Card. Fail.* 21, 973–980. doi: 10.1016/j.cardfail. 2015.09.017

Nie, Y. F., Hu, J., and Yan, X. H. (2015). Cross-talk between bile acids and intestinal microbiota in host metabolism and health. *J. Zhejiang Univ. Sci. B* 16, 436–446. doi: 10.1631/jzus.B1400327

Oliphant, K., Ali, M., D'Souza, M., Hughes, P. D., Sulakhe, D., Wang, A. Z., et al. (2021). *Bacteroidota* and *Lachnospiraceae* integration into the gut microbiome at key time points in early life are linked to infant neurodevelopment. *Gut Microbes* 13:1997560. doi: 10.1080/19490976.2021.1997560

Pasini, E., Aquilani, R., Testa, C., Baiardi, P., Angioletti, S., Boschi, F., et al. (2016). Pathogenic gut flora in patients with chronic heart failure. *JACC Heart Fail* 4, 220–227. doi: 10.1016/j.jchf.2015.10.009

Perino, A., Demagny, H., Velazquez-Villegas, L., and Schoonjans, K. (2021). Molecular physiology of bile acid signaling in health, disease, and aging. *Physiol. Rev.* 101, 683–731. doi: 10.1152/physrev.00049.2019

Samsamshariat, S. A., Samsamshariat, Z. A., and Movahed, M. R. (2005). A novel method for safe and accurate left anterior descending coronary artery ligation for research in rats. *Cardiovasc. Revasc. Med.* 6, 121–123. doi:10.1016/j.carrev.2005.07.001

Sangeethadevi, G., Sathibabu Uddandrao, V. V., Jansy Isabella, R., Saravanan, G., Ponmurugan, P., Chandrasekaran, P., et al. (2022). Attenuation of lipid metabolic abnormalities, proinflammatory cytokines, and matrix metalloproteinase expression by biochanin-A in isoproterenol-induced myocardial infarction in rats. *Drug. Chem. Toxicol.* 45, 1951–1962. doi: 10.1080/01480545.2021.1894707

Savarese, G., Becher, P. M., Lund, L. H., Seferovic, P., Rosano, G., and Coats, A. (2023). Global burden of heart failure: A comprehensive and updated review of epidemiology. *Cardiovasc. Res.* 118, 3272–3287. doi: 10.1093/cvr/cvac013

Tang, W., Li, D. Y., and Hazen, S. L. (2019). Dietary metabolism, the gut microbiome, and heart failure. *Nat. Rev. Cardiol.* 16, 137–154. doi: 10.1038/s41569-018-0108-7

Wahlström, A., Sayin, S. I., Marschall, H. U., and Bäckhed, F. (2016). Intestinal crosstalk between bile acids and microbiota and its impact on host metabolism. *Cell Metab.* 24, 41–50. doi: 10.1016/j.cmet.2016.05.005

Wang, M. N., Cao, Y. G., Wei, Y. X., Ren, Y. J., Liu, Y. L., Chen, X., et al. (2022). Saffloflavone, a new flavonoid from the flowers of *Carthamus tinctorius* L. and its cardioprotective activity. *Nat. Prod. Res.* 36, 3317–3323. doi: 10.1080/14786419.2020. 1855167

Wang, X., Li, W., Zhang, Y., Sun, Q., Cao, J., Tan, N., et al. (2022). Calycosin as a novel PI3K activator reduces inflammation and fibrosis in heart failure through AKT-IKK/STAT3 axis. Front. Pharmacol. 13:828061. doi: 10.3389/fphar.2022.828061

Wang, Y., Wang, Q., Li, C., Lu, L., Zhang, Q., Zhu, R., et al. (2017). A review of chinese herbal medicine for the treatment of chronic heart failure. *Curr. Pharm. Des.* 23, 5115–5124. doi: 10.2174/1381612823666170925163427

Wang, Z., Liu, C., Wei, J., Yuan, H., Shi, M., Zhang, F., et al. (2024). Network and experimental pharmacology on mechanism of yixintal regulates the TMAO/PKC/NF-kB signaling pathway in treating heart failure. *Drug Design Dev. Therapy* 18, 1415–1438. doi: 10.2147/DDDT.S.448140

Winston, J. A., and Theriot, C. M. (2020). Diversification of host bile acids by members of the gut microbiota. *Gut Microbes* 11, 158–171. doi: 10.1080/19490976. 2019 1674124

Wohlfahrt, P., Jenča, D., Stehlik, J., Melenovský, V., Mrázková, J., Staněk, V., et al. (2023). Heart failure-related quality-of-life impairment after myocardial infarction. *Clin. Res, Cardiol.* 112, 39–48. doi: 10.1007/s00392-022-02008-z

Yang, C., Li, X., Hu, M., Li, T., Jiang, L., and Zhang, Y. (2024). Gut microbiota as predictive biomarker for chronic heart failure in patients with different nutritional risk. *J. Cardiovasc. Transl. Res.* 17, 1240–1257. doi: 10.1007/s12265-024-10529-3

Yu, W., Jiang, Y., Xu, H., and Zhou, Y. (2023). The interaction of gut microbiota and heart failure with preserved ejection fraction: From mechanism to potential therapies. Biomedicines 11:442. doi: 10.3390/biomedicines11020442

Yuzefpolskaya, M., Bohn, B., Nasiri, M., Zuver, A. M., Onat, D. D., Royzman, E. A., et al. (2020). Gut microbiota, endotoxemia, inflammation, and oxidative stress in patients with heart failure, left ventricular assist device, and transplant. *J. Heart Lung Transplant* 39, 880–890. doi: 10.1016/j.healun.2020.02.004

Zhang, Q. L., Chen, X. H., Zhou, S. J., Lei, Y. Q., Huang, J. S., Chen, Q., et al. (2023). Relationship between disorders of the intestinal microbiota and heart failure in infants with congenital heart disease. *Front. Cell Infect. Microbiol.* 13:1152349. doi: 10.3389/fcimb.2023.1152349

Zhang, S., Zhou, J., Wu, W., Zhu, Y., and Liu, X. (2023). The role of bile acids in cardiovascular diseases: From mechanisms to clinical implications. *Aging Dis.* 14, 261–282. doi: 10.14336/AD.2022.0817

Zhang, Y., Chen, L., Hu, M., Kim, J. J., Lin, R., Xu, J., et al. (2020). Dietary type 2 resistant starch improves systemic inflammation and intestinal permeability by modulating microbiota and metabolites in aged mice on high-fat diet. *Aging* 12, 9173–9187. doi: 10.18632/aging.103187

Zuo, L., Chuang, C. C., Hemmelgarn, B. T., and Best, T. M. (2015). Heart failure with preserved ejection fraction: Defining the function of ROS and NO. *J. Appl. Physiol.* 119, 944–951. doi: 10.1152/japplphysiol.01149.2014